The subtle tetramorphism of $MePh_3P^+I_3^-$

Hong Chow,[a] Philip A. W. Dean,[b] Donald C. Craig,[a] Nigel T. Lucas,[a] Marcia L. Scudder[a] and Ian G. Dance*[a]

[a] *School of Chemistry, University of New South Wales, Sydney NSW 2052, Australia*
[b] *Department of Chemistry, University of Western Ontario, London, ON N6A 5B7, Canada*

Received (in Montpellier, France) 19th August 2002, Accepted 10th December 2002
First published as an Advance Article on the web 26th February 2003

The crystallisation and crystal structures of three new crystal forms of $MePh_3P^+I_3^-$ are described, bringing to four the number of polymorphs of this compound. Crystallisations were from alcohols, mixed alcohols, and dichloromethane, and are reproducible. There are strong similarities between all four of the crystal packing arrangements, which are solvent-free. In all structures the $MePh_3P^+$ cations associate in two-dimensional nets using edge-to-face, offset-face-to-face, and methyl-to-face motifs, and the I_3^- ions lie between these nets, with subtle variations in structure caused by sliding displacements of relatively constant cation-anion assemblies. The related compound $EtPh_3P^+I_3^-$ has very similar crystal packing. The interactions between the I_3^- and $MePh_3P^+$ are mainly C–H···I, with some phenyl faces parallel to I_3^-. The major electrostatic component of the lattice energy is associated with the occurrence of I_3^- ions against the faces of nets of cations, consistent with this structural feature being the most invariant aspect of the crystal packing, while the structural variability is associated with the less stabilising cation···cation motifs. It appears that these crystals provide a good example of a system where shape is not a dominant feature in crystal packing, and that the tetramorphs represent almost equi-ergic local minima in a relatively deep section of the lattice energy hypersurface. The crystal packing of $(MePh_3P^+)_2I_8^{2-}$ is similar.

Introduction

Polymorphism, the crystallisation of one compound to yield different crystal structures, is a phenomenon of fundamental significance and curiosity,[1,2] and industrial concern.[3] For structurally molecular compounds containing neutral or charged species the formation conditions and the structures of alternative crystal forms provide data about crystallisation dynamics and crystal packing energies. The transformation of a solution to a crystal[4] is still surrounded by many questions, even for common and well-known compounds. Polymorphs are usefully regarded as crystal packing isomers, and as such they yield views of geometrical arrangements that presumably have similar crystal packing energies, and provide valuable calibration points for the calculation of intermolecular energies, and for simulations and predictions of crystal structure.

It has been suggested that polymorphism could be much more extensive than currently recognised, mainly because most new compounds are crystallised only once (to obtain a crystal and molecular structure) without variation of the crystallisation conditions. One objective of our research is to uncover polymorphs. We commonly investigate the crystallisation of our compounds in different ways, and, particularly where iodides and polyiodides are involved, have found a number of sets of polymorphs.[5] The subtleties of crystallisation phenomena have also been very evident to us, as unreproducible crystallisations.[6] One aspect of this is the presence of other species in the crystallisation solution: reversible adsorption at growing crystal faces is established as an influential process,[7] and templating[8] and chaperone[9] phenomena may occur.

In this paper we describe the tetramorphs of the compound $MePh_3P^+I_3^-$. One crystal form, **1**, is already in the literature[10] (CSD refcode VISKAJ). We have crystallised three new forms,

Table 1 New crystal data for $MePh_3P^+I_3^-$

	2	**3**	**4**
Formula	$C_{19}H_{18}PI_3$	$C_{19}H_{18}PI_3$	$C_{19}H_{18}PI_3$
M	658.0	658.0	658.0
Crystal system	Monoclinic	Triclinic	Orthorhombic
Space group	$P2_1/c$	$P\bar{1}$	$Pbca$
a/Å	19.770(8)	11.957(7)	14.650(3)
b/Å	11.978(3)	12.089(8)	16.525(3)
c/Å	18.715(8)	16.199(9)	18.089(4)
α/°	90	87.50(3)	90
β/°	107.10(3)	75.27(3)	90
γ/°	90	69.40(3)	90
U/Å^3	4236(4)	2117(2)	4379(2)
Z	8	4	8
μ_{Mo}/mm^{-1}	4.45	4.46	4.31
Unique reflect.	5650	5866	3846
Obsd reflect.	2342	2998	1554
R_{merge}	0.078	0.019	—
R	0.068	0.048	0.046
R_w	0.083	0.062	0.050

Table 2 Unit cell dimensions and space groups for the tetramorphs of $MePh_3P^+I_3^-$

Crystal form	Space group	Unit cell dimensions (in Å and °)
1	$Pbca$	$a = 11.82$, $b = 19.88$, $c = 18.00$
2	$P2_1/c$	$a = 19.77$, $b = 11.98$, $c = 18.72$, $\beta = 107.1$
3	$P\bar{1}$	$a = 11.96$, $b = 12.09$, $c = 16.20$, $\alpha = 87.5$, $\beta = 75.3$, $\gamma = 69.4$
4	$Pbca$	$a = 14.65$, $b = 16.53$, $c = 18.09$

 DOI: 10.1039/b208112a

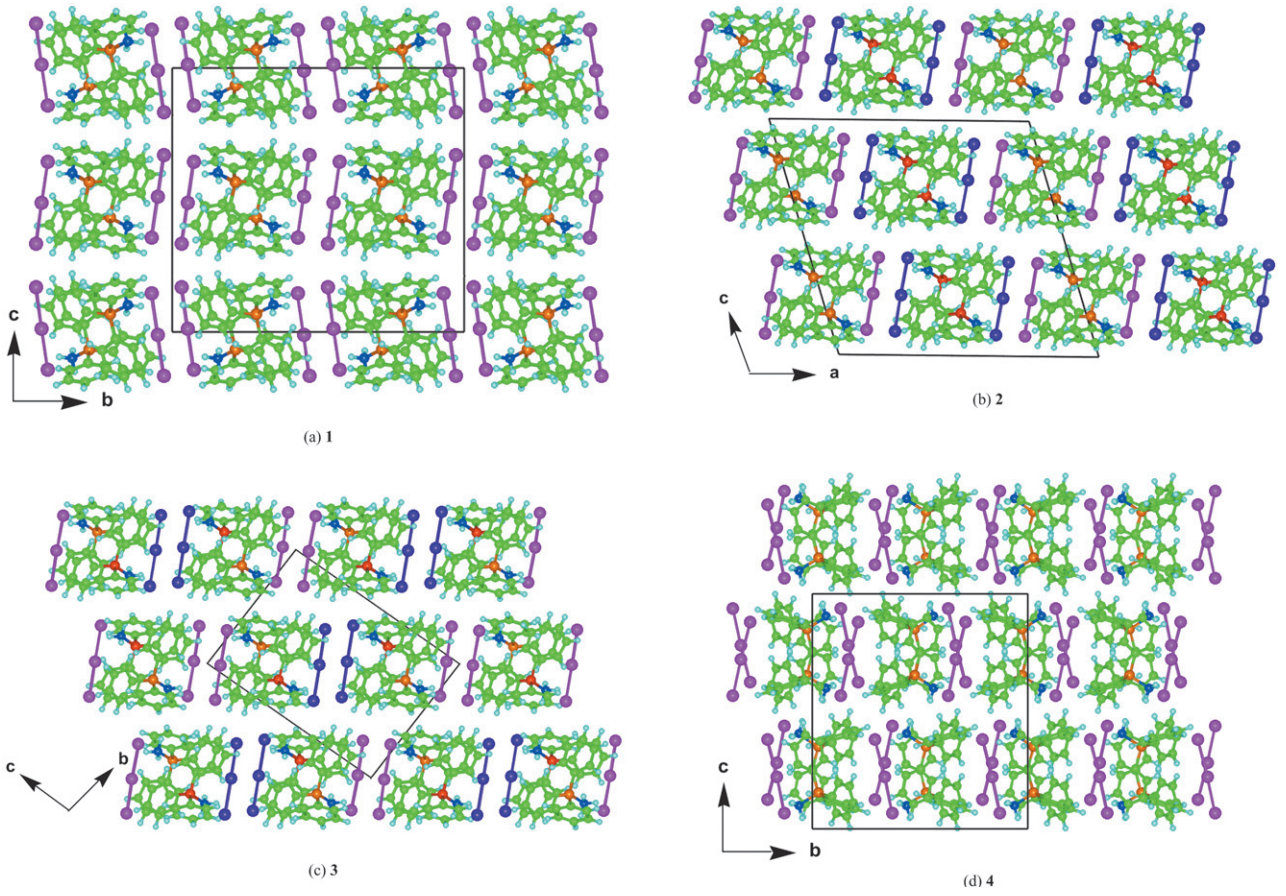

Fig. 1 Comparative projections of the four crystal structures of $MePh_3P^+I_3^-$, emphasising their similar crystal packing. (a) Structure **1** in space group *Pbca*. (b) Structure **2** in space group $P2_1/c$. (c) Structure **3** in space group $P\bar{1}$. (d) Structure **4** in space group *Pbca*. In each case there are chains of cations that run parallel to the projection direction. In (b) and (c) the two independent cations are distinguished by red and orange P atoms, while the two independent anions are coloured purple and magenta.

2, **3** and **4**. We describe the crystal packing of the four forms and explain the rather subtle differences that occur, in the context of the structures of related compounds and motifs. We also offer some interpretation of this instance of polymorphism.

Experimental

Crystallisations

Crystallisation of 1. Crystals of **1** were obtained from solutions in CH_2Cl_2 (30–76 mM) following infusion of hexane or 2-PrOH at *ca.* 0 °C, or evaporation after addition of 2-PrOH. **1** was also obtained from solutions in $CHCl_3$ after slow infusion of hexane or EtOH at 0 °C.

Crystallisation of 2 and 3 by a logical method. $MePh_3P^+I^-$ (20 mg, 0.05 mmol) and I_2 (7.5 mg, 0.03 mmol) were dissolved in 15 mL of 2-PrOH, with slight heating. After a few days, crystals had formed in a small amount and were separated by decantation. The solvent was allowed to evaporate slowly from the mother liquor. After *ca.* 3 months, a mixture of brown prisms (the minor component) and yellow flat plates (major component) had formed. Diffraction measurements showed that the first and the second crops of crystals were the same mixture of **2** (yellow flat plates) and **3** (brown prisms).

Serendipitous crystallisation of 2 and 3. Equal volumes of solutions of SnI_4 in EtOH (5 mM), phthalic acid in EtOH (5 mM) and $MePh_3P^+Br^-$ in MeOH (10 mM) were mixed. After slow evaporation a mixture of orange plates (**2**) and brown crystals (**3**) had formed.

Crystallisation of 4. $MePh_3P^+I^-$ (20 mg, 0.05 mmol) and I_2 (7.5 mg, 0.03 mmol) were dissolved in 15 mL of EtOH–MeOH (2:1 by volume). Solvent was allowed to evaporate slowly over *ca.* 3 months, when yellow-brown crystals were formed, as

Table 3 Symmetry elements generating the crystal packing features for the tetramorphs of $MePh_3P^+I_3^-$

Crystal form	Space group	Symmetry generating the cation chain(s)	Symmetry generating the cation net from cation chains
1	*Pbca*	2_1 screw axis parallel to *a* at $b = 1/4$, $c = 0$	Glide plane parallel to the *ac* plane at $b = 1/4$ with translation along *c*
2	$P2_1/c$	2_1 screw axis parallel to *b* at $a = 0$, $c = 1/4$	Inversion centres
3	$P\bar{1}$	Translation along *a* of the pair of independent cations	Inversion centres
4	*Pbca*	Glide plane parallel to the *ab* plane at $c = 1/4$ with translation along *a*	Inversion centres

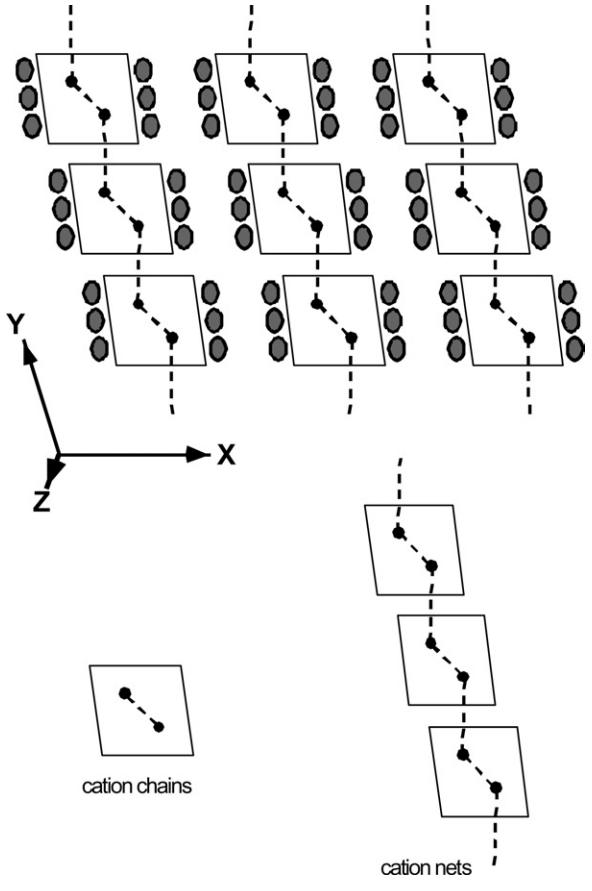

Scheme 1

both prisms and plates. Both types of crystals were shown by diffraction to be **4**. This crystal form was obtained consistently by crystallisation of $MePh_3P^+I_3^-$ from pure MeOH, 1-PrOH or 2-PrOH, provided that excess (up to 50%) $MePh_3P^+I^-$ was present. On only one occasion was **4** crystallised from an alcohol (MeOH) in the absence of excess $MePh_3P^+I^-$. Attempted crystallisation of $MePh_3P^+I_3^-$ from MeOH with excess I_2 yielded an oil at ambient temperature.

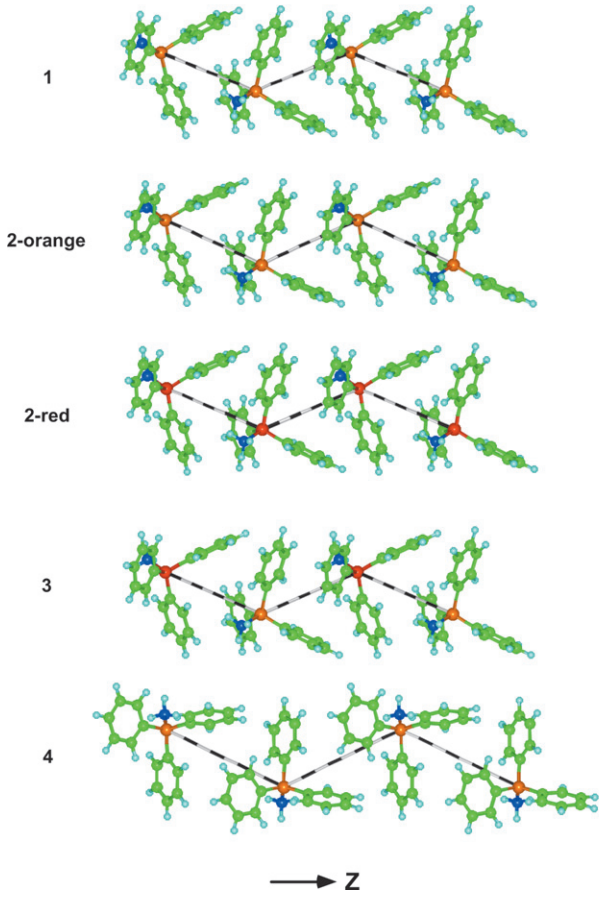

Fig. 2 The five different chains of $MePh_3P^+$ that occur in **1**, **2**, **3** and **4** (see Table 3 for symmetry elements that generate the chains). The P···P distances and P···P···P angles are: 6.53 Å, 130° for **1**; 6.73 Å and 126° for **2**-orange; 6.65 Å and 128° for **2**-red; 6.65 alternating with 6.69 Å, 127° for **3**; and 8.14 Å and 128° for **4**.

Crystallisation of 2 alone. Only one experiment yielded **2** alone. A solution of $MePh_3P^+I_3^-$ in $CHCl_3$ (38 mM) was infused with MeOH at *ca.* 0 °C for 1 week without crystallisation. Subsequent slow evaporation at *ca.* 20 °C over 3 weeks yielded **2**.

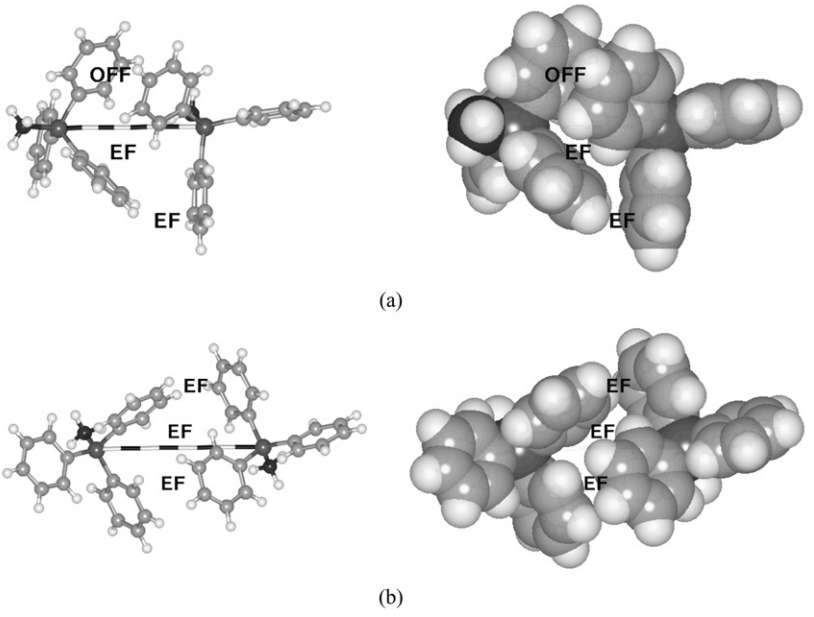

Fig. 3 (a) The recurring embrace between $MePh_3P^+$ along the cation chains in **1**, **2** and **3**. The principal features are the OFF and two EF interactions, as marked. (b) The embrace found in **4** comprised of three EF interactions.

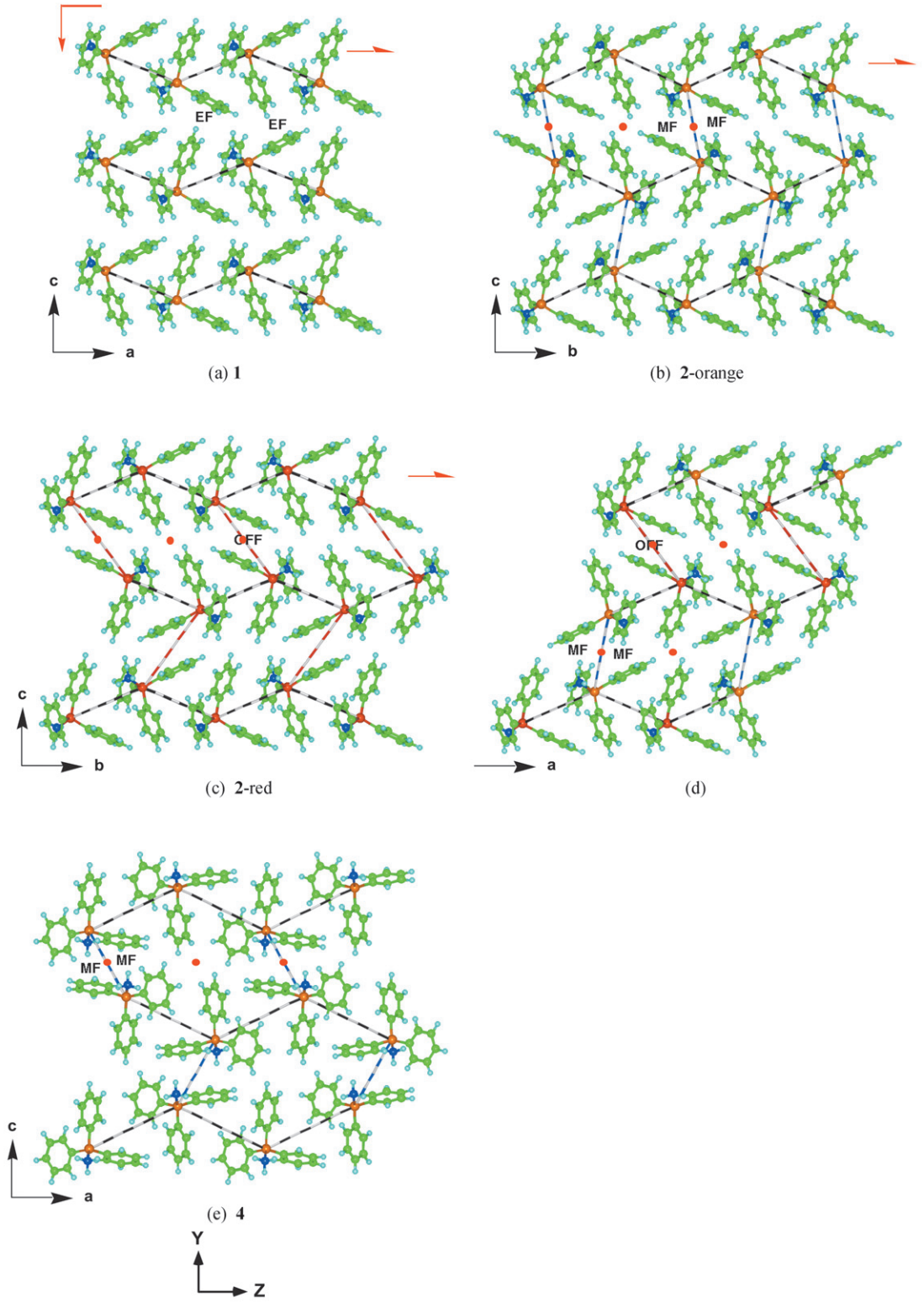

Fig. 4 The nets of interacting $MePh_3P^+$ ions in **1**, **2**, **3** and **4**, occurring in the *YZ* plane (defined in Scheme 1). Black dashed lines identify the cation chains. (a) In **1** all cations have their methyl groups directed to the left. The two different EF interactions between chains are labelled. (b) In the **2**-orange net alternating chains of cations run in opposing directions and are related by centres of symmetry (marked as red dots). Between chains there are approximately hexagonal regions. The interchain interactions (blue dashed lines) are comprised of a pair of centrosymmetric methyl-to-phenyl-face $(MF)_2$ interactions, and there are no interchain phenyl···phenyl interactions. (c) The **2**-red net is similar to the **2**-orange net in (b), being a result of the same symmetry operations, but there is larger lateral shift between adjacent chains, leading to more distorted hexagonal regions. The interchain interactions here are good centrosymmetric OFF (red dashed lines). (d) The net of $MePh_3P^+$ ions in **3**, which is a composite of the arrangements shown in (b) and (c). The upper part of the figure shows the more distorted hexagonal regions, completed by good OFF interactions (red dashed lines). The lower pair of chains illustrates the more regular hexagonal region, with $(MF)_2$ interactions between chains (blue dashed lines). (e) The net of cations in **4**. The blue striped connectors are $(MF)_2$ interactions.

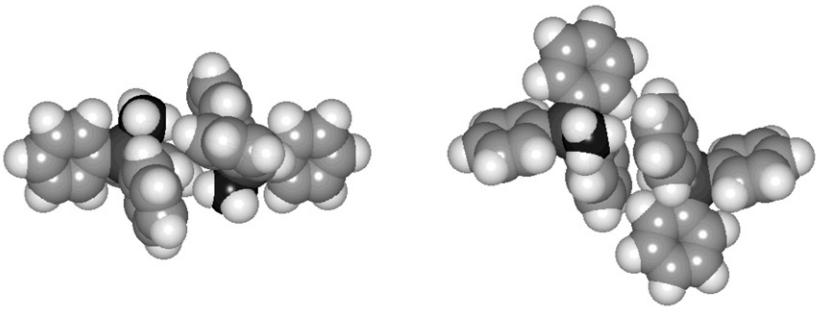

Fig. 5 The centrosymmetric double methyl-to-face $(MF)_2$ interaction (the blue dashed lines in Fig. 4). The methyl hydrogen atoms were included in calculated positions assuming a staggered configuration, which positions one hydrogen atom directly over the phenyl face. The two views are related by 90° rotation around the horizontal axis.

Mixture of 1 and 2. One experiment yielded a mixture of **1** and **2**. Hexane was diffused into a solution of $MePh_3P^+I_3^-$ in acetone (76 mM) at *ca.* 0 °C for 1 week, yielding **1** as red prisms and **2** as orange-red rectangular prisms.

Crystal structures

Data were collected at ambient temperature using a Nonius CAD4 diffractometer with graphite monochromated MoKα radiation ($\lambda = 0.7107$ Å). Iodine atoms were refined anisotropically, while each phenyl group was refined with thermal motion described by a 12 parameter TL group (where T is the translation tensor and L is the libration tensor) with its origin of libration at P. Hydrogen atoms of the cations were incorporated in calculated positions and were included in the group thermal for that ring. For **2**, residual electron density in the region of the iodine atoms suggested minor disorder or stacking faults. Disorder was discounted because it involved atom interference: stacking faults with displacements of about ±1.3 Å roughly parallel to the triiodide ions, each with frequencies of 5 percent, were included. This reduced *R* from 0.10 to 0.068. Details of data collection and refinement for all three structures are given in Table 1. CCDC reference numbers 192040–42. See http://www.rsc.org/suppdata/nj/b2/b208112a/ for crystallographic files in CIF or other electronic format.

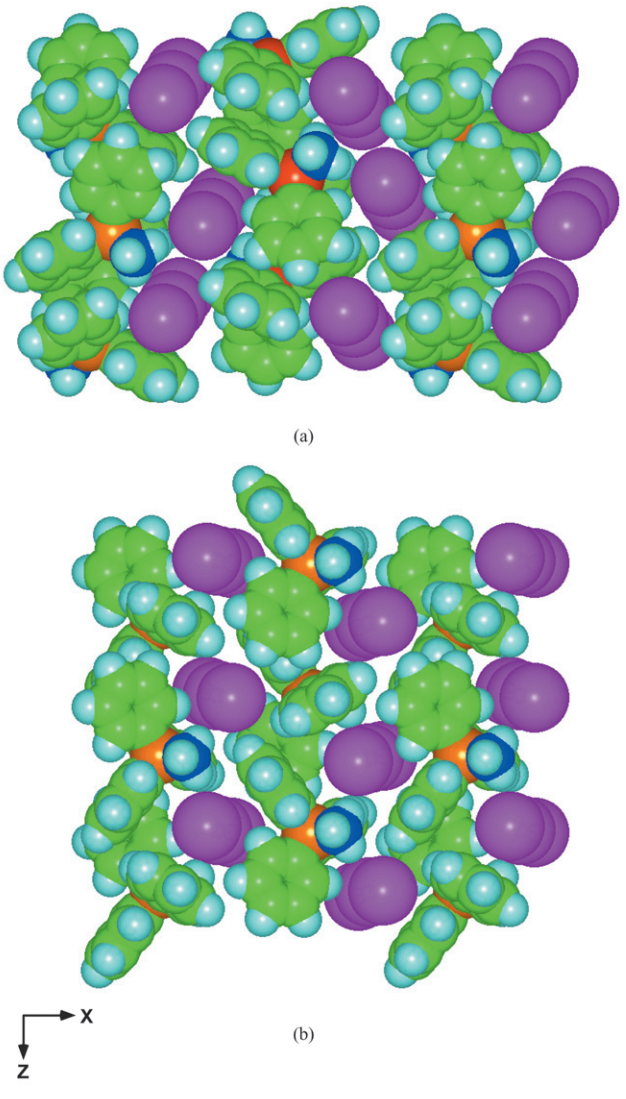

Fig. 6 The alternation of cations chains and I_3^- ions along the *X* direction (see Scheme 1). (a) The arrangement that occurs with very little variation in crystals **1**, **2**, and **3**: crystal **2** is drawn. (b) Crystal **4**.

Results

$MePh_3P^+I_3^-$ in crystal form **1** was obtained by recrystallisation from dichloromethane, in the original work,[10] and by us. Crystal forms **2** and **3** were obtained together by crystallisation from methanol–ethanol mixtures, and separate crystallisation of each form is difficult with **2** obtained alone in only one crystallization, from chloroform–methanol. Forms **2** and **3** were also obtained together from a long-standing mixture in methanol–ethanol where hydrolysis and oxidation of SnI_4 was the source of I_3^-, and phthalic acid and bromide were also present in solution. **2** and **3** are near concomitant polymorphs.[2] Crystallisation of $MePh_3P^+I_3^-$ from methanol, 1-propanol or 2-propanol yielded crystal form **4** when excess $MePh_3P^+I_3^-$ was present. Crystal form **1** was reported to be deep violet, while **2**, **3** and **4** were yellow-brown.

The lattice dimensions and space groups of the tetramorphs (Table 2) show some similarities. The unit cell dimensions of **1** and **2** are similar (with interchange of *a* and *b*); **1**, **2** and **3** have a 12 Å axis, and **1**, **2** and **4** have an axis of *ca.* 18 Å. The orthorhombic structures **1** and **4** have one cation and one anion as the asymmetric unit, while **2** and **3** have two cations and two anions as the asymmetric unit. The relationships will be more evident in the descriptions of the crystal packing.

Crystal packing

Projections of each structure, oriented to reveal the similarities, are contained in Fig. 1. In this and subsequent figures methyl carbon atoms are coloured blue, and in **2** and **3** the two cations in the asymmetric unit are distinguished with orange and red phosphorus atoms and the two distinct I_3^- ions are coloured magenta and purple. Symmetry elements generating the various crystal packing features are given in Table 3.

The most obvious feature is the similarity of these four crystal packing arrangements. However, closer examination also reveals the clear but subtle differences between the four

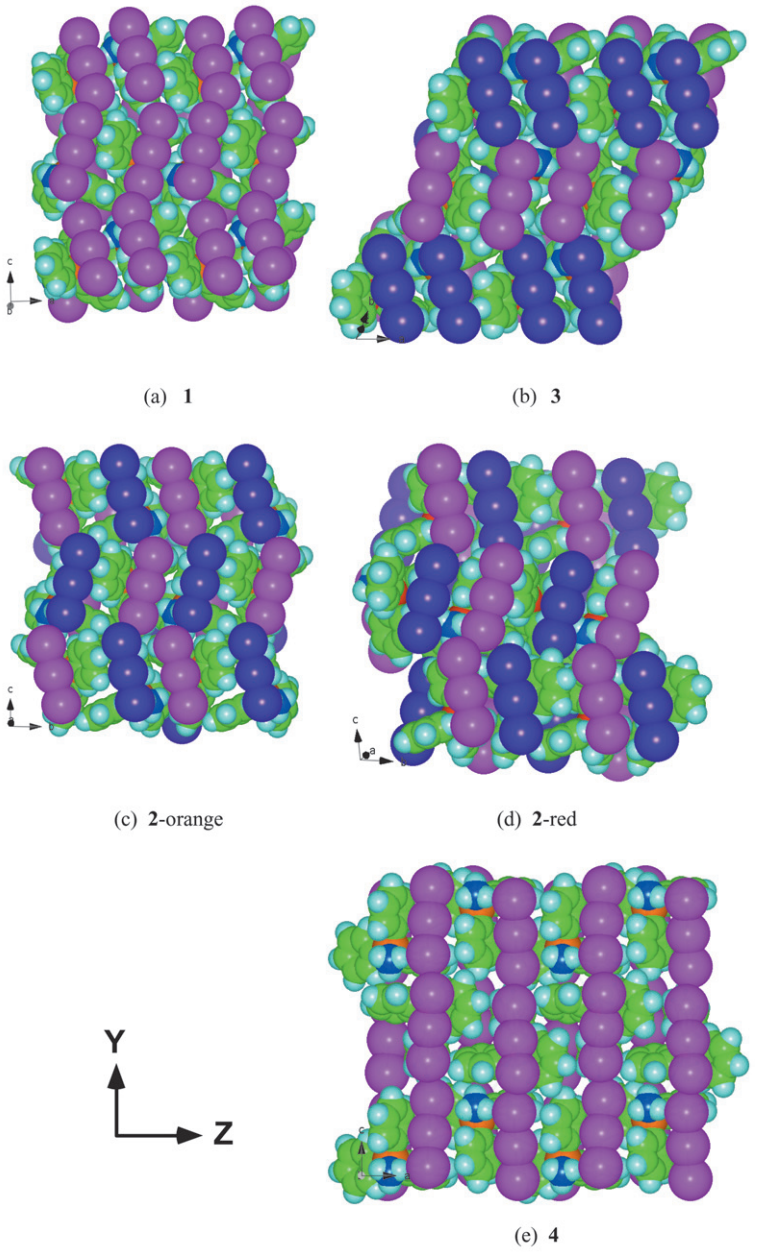

Fig. 7 Comparative space-filling views of the tetramorphs, approximately normal to the cation nets, with the associated I_3^- ions included. This is essentially the same orientation as in Fig. 4. For **1**, **2** and **3**, the view directions have been selected to emphasise the similarity of the central row of anions in each. The shortest distance between I_3^- ions is 4.1 Å in **1**, **2** and **3**, and 4.3 Å in **4**.

tetramorphs. In order to develop the description and analyses of these structures, we define in Scheme 1 some structural components and elements, and define the cartesian directions *X*, *Y*, *Z* that are common to the four crystal packings. The variations in the structures are variations in juxtaposition of these elements. Axes *X*, *Y*, *Z*, used throughout the following descriptions, are not the crystal axes of the individual crystals, but are new axes defined in terms of the common crystal packing features. The cations occur in chains defining the *Z* direction: these chains are clearly evident as green boxes in Fig. 1, and are marked as boxes in Scheme 1. These chains are further linked along the *Y* direction into cation nets. The I_3^- ions are located on either side of the cation chains. The lengths of the I_3^- ions are similar to the dimension of the cation box in the *Y* direction.

Some subtle points can be discerned in Fig. 1. Crystals **2** and **3** appear to be virtually identical in this view, but the differences occur in the crystallographic differentiation of the cations and anions: this is elaborated below. Crystal **1** is very similar to **2** and **3**, except that the angle between *X* and *Y* is less obtuse. Crystal **4** varies in the position of the cation centres in the cation chains and in the placement of the anions beside the chains. Next we describe the cation chains and nets in more detail.

Cation···cation interactions: chains and nets

Details of the chains of $MePh_3P^+$ ions that run along the *Z* direction are presented in Fig. 2. There are two crystallographically independent chains of cations in **2**, labelled **2**-orange and **2**-red according to the P-colouration in Fig. 2, and the one chain type in **3** contains alternating crystallographically independent cations.

Fig. 2 shows that the four distinct chains of $MePh_3P^+$ in **1**, **2** and **3** are virtually identical. Each of these chains is generated by repetition of the embrace motif shown in Fig. 3(a), in which four phenyl groups (two from each cation) form one offset-face-to-face (OFF) pair and two edge-to-face (EF) pairs. The

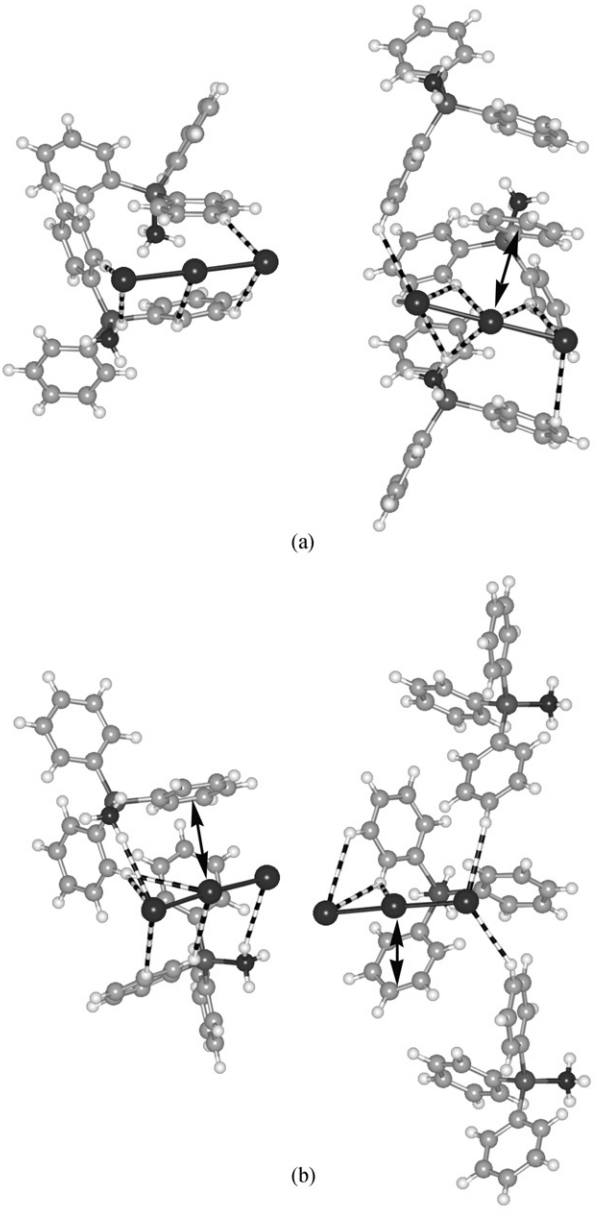

Fig. 8 (a) Representations of the $MePh_3P^+$ ions surrounding one I_3^- ion in **1**, **2** and **3**. C–H···I interactions (black and white connectors) and the I_3^--to-phenyl face interaction (black arrow) are marked. (b) The corresponding views for **4**. Note that there are now two I_3^--to-phenyl face interactions.

methyl groups are not involved. The chain in **4** is different from that in the other three structures, with a longer P···P distance. The embrace in **4** is a composite of three EF interactions [Fig. 3(b)].

Despite the appearance of Fig. 1, these chains of cations are not isolated from each other and are connected by embrace motifs along the *Y* direction, forming the cation nets in the *YZ* crystal packing plane. These nets of cations are appreciably folded in **1**, slightly puckered in **2** and **3**, and slightly folded in **4** (see Fig 1). Details of the interactions between the chains to form the nets are illustrated in Fig. 4 (see Table 3 for the propagating symmetry operations).

The differences between the tetramorphs are clearly evident in Fig. 4. There are four different nets of interactions between $MePh_3P^+$ ions in Fig. 4(a), (b), (c) and (e), while Fig. 4(d) is a combination of (b) and (c). The extent of the offset of adjacent chains can be assessed by the large intra-hexagon P···P···P angle (not along the chain). The value is 127° and 150° for **2**-orange and **2**-red, respectively, 126° and 151° for the composite net in **3**, and for **4**, the angle is intermediate, at 145°. The pseudo-hexagonal nets of interacting cations are reminiscent of those formed by Ph_4P^+ cations.[11] A detailed view of the centrosymmetric $(MF)_2$ motif that occurs in the nets of **2**-orange, **3** and **4** is provided in Fig. 5.

Cation···anion arrangements

Along the *X* direction in the crystal packing there are alternating layers of cation nets and I_3^- ions. In crystals **1**, **2** and **3** the relationships between cation chains and the intermediate I_3^- ions along the *X* directions are effectively invariant. Fig. 6(a) shows this relationship, as the *YZ* layers viewed down the *Y* direction. This aspect is slightly different in **4**, as shown in Fig. 6(b).

As already indicated in Fig. 1, the structures differ in the stacking of the cation chains plus I_3^- units (Fig. 6) along the *Y* direction. Fig. 7 describes these relationships in more detail, with views of the *YZ* plane of each structure, including one cation net and the I_3^- ions associated with it. The view direction is essentially the same as that of the cation nets in Fig. 4, but now the I_3^- ions are included, and the representation is space-filling. This allows further insight into the similarities and the differences between the tetramorphs. The differences between **1**, **2** and **3** are subtle, but evident, while the packing in **4** has some clear differences. There are no significant close contacts (< 4.1 Å) between I_3^- ions in any of these crystals.

Each I_3^- ion is surrounded by five cations in all four structures. The immediate contacts are primarily C–H···I, and include H from both the phenyl rings and the methyl group. There is one very well-formed I_3^--to-phenyl face interaction in **1**, **2** and **3** and two such interactions in **4**, which are evident in Fig. 6(a) and 6(b). Fig. 8(a) shows two views of the anion environment common to **1**, **2** and **3**, where some cations have been omitted to reveal details of the individual C–H···I interactions. The corresponding views for **4** are shown in Fig. 8(b).

The similar crystal structure of $EtPh_3P^+I_3^-$

Before proceeding to the interpretation of our results, we introduce a relevant and informative observation, which is the crystal structure of the ethyl derivative, $EtPh_3P^+I_3^-$ (CSD refcodes JULGEC[12] and JULGEC01[13]). Relevant aspects of this structure are shown in Fig. 9, which illustrates the close similarities to the structures of **1**, **2** and **3** for $MePh_3P^+I_3^-$, as well as the differences. The projection of the crystal lattice [Fig. 9(a)] is remarkably similar to those for **2** and **3** [Fig. 1(b) and (c)]. The occurrence of cation chains and the recurring embrace along the chains, is virtually the same as those in **1**, **2** and **3**, as is evident by comparison of Fig. 9(b) with Fig. 2. This is possible because the methyl or ethyl groups are not involved in these interactions. However, the ethyl groups do influence the two-dimensional net of cations and the arrangement shown in Fig. 9(c) is different from any in Fig. 4.

Interpretation

We have described the structures and intermolecular interactions for the tetramorphs, and their similarities and minor differences. A more difficult task is interpretation of the structures and generation of hypotheses about why and how the tetramorphs have formed. What can be learned from the existence of these crystals? Significant questions occur for the measured structures of the crystals, and for the unmeasured desolvation and nucleation phenomena that generated them.

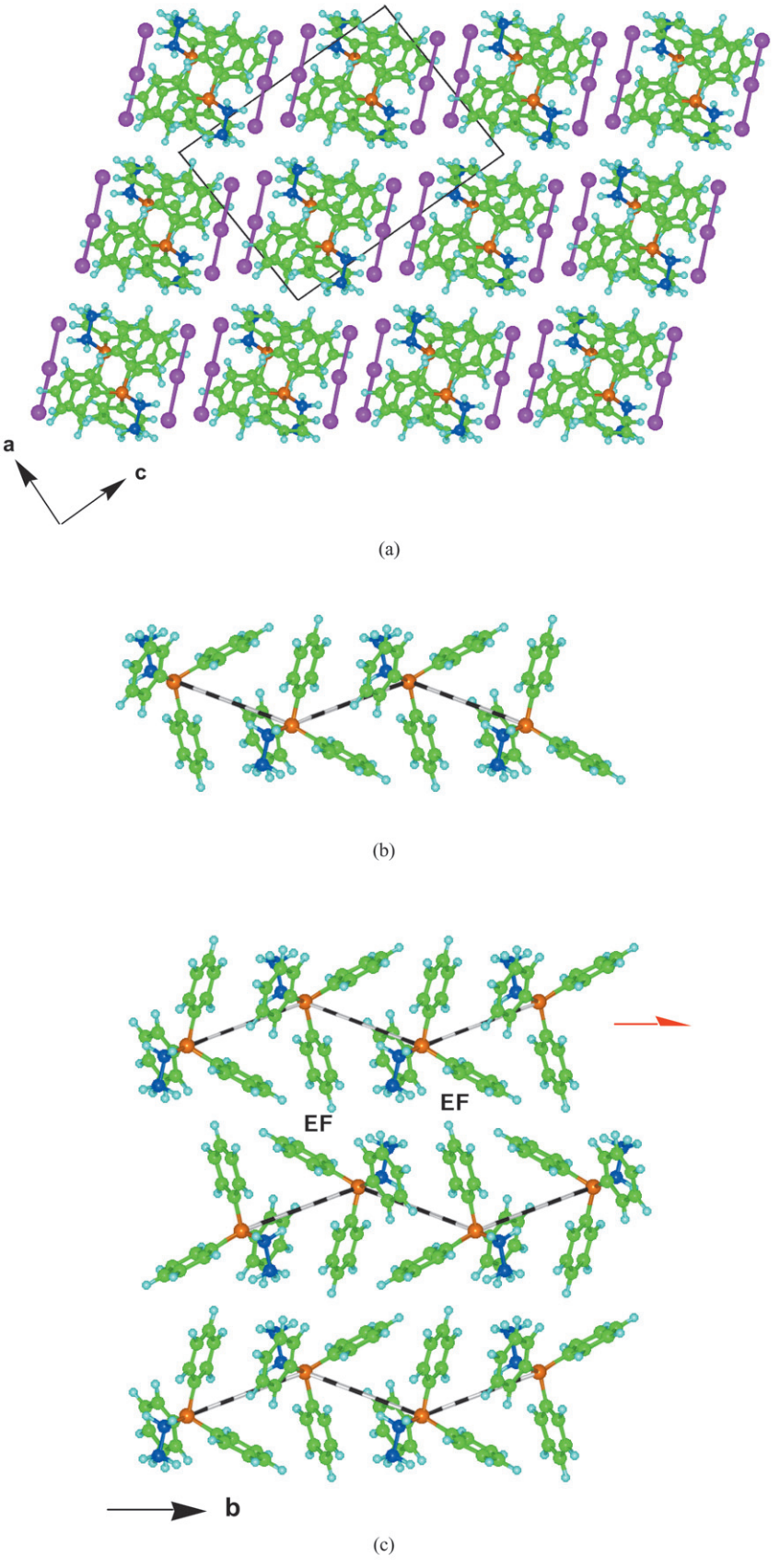

Fig. 9 Aspects of the crystal packing in $EtPh_3P^+I_3^-$ (JULGEC01, space group $P2_1/n$), for comparison with the packing of $MePh_3P^+I_3^-$: ethyl C atoms are coloured blue. (a) Projection along the columns in which the chains of cations are aligned similarly to those in Fig. 1(b), (c). (b) The chain of cations, very similar to those in Fig. 2(a), (b), (c), (d). (c) The net of cations, which is subtly different from any of the nets shown in Fig. 4.

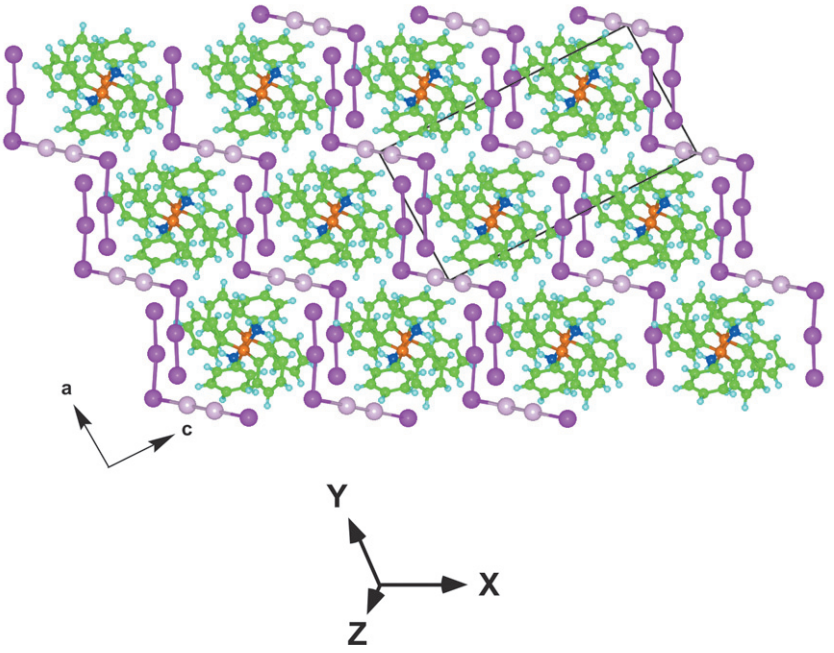

Fig. 10 Projection of the crystal structure of $(MePh_3P^+)_2I_8^{2-}$ (ZEZDIR, space group $P2_1/n$), oriented to show the similar crystal packing to that in the structures of **1**, **2** and **3**. The I_3 segments on the edges of the columns of cations are linked by I_2 segments (pale pink), thereby forming bonded linkages in the *Y* direction.

It is reasonable to consider also $EtPh_3P^+I_3^-$ which, while not a strict polymorph of $MePh_3P^+I_3^-$, does demonstrate the same crystal packing features. The occurrence of five instances of the same type of crystal packing indicates that this overall crystal packing, generalised in Scheme 1, is appreciably more stable than alternatives: for instance, an alternative crystal packing could have the cation nets (*YZ* plane) rotated relative to each other about the *X* axis. Therefore, the qualitative view of the crystal packing polymorphism is that there is a relatively deep potential energy well in the lattice energy hypersurface, within which there are four (or more) local minima with similar energies. While the energies of intermolecular interactions have not been estimated in this work, it is clear that the electrostatic stabilisation of the I_3^- ions against the faces of the net of $MePh_3P^+$ cations (as in Fig. 7) will be a major component of the lattice energy. This is consistent with the observation that the $MePh_3P^+\cdots I_3^-$ interactions are the most invariant aspect of the crystal packing. Structural variability occurs in the cation chains and nets, where the motifs have a destabilising electrostatic energy superimposed on the van der Waals stabilisation of the cation motifs. The variations in structure are sliding displacements of relatively constant cation-anion assemblies.

So, our interpretation of the occurrence (as opposed to formation) of the tetramorphic crystals is that their structures are controlled principally by electrostatic influences, and that the variability occurs in the less stabilising regions of the structures, and constancy in the more stabilising regions. It is significant that the anion I_3^- is small and not shape-awkward, and so shape is not a controlling influence in the polymorphic structures. The C–H···I interactions can be and are formed in a variety of ways around I_3^-.

Regarding the crystallisation phenomena, the influence of solvent appears to be relatively minor, except for the fact that dichloromethane has yielded only **1** so far. It is worth noting that structures **2** and **3** are the most similar, and that these two crystals grow together as concomitant polymorphs in almost all of our crystallisations (from MeOH plus EtOH, and from 2-PrOH) so far. We speculate that the nucleation cluster is relative small, possibly just one cation and one anion, and that growth is primarily controlled by association of these along the crystal packing *X* direction. This would be growth by addition to the faces viewed in Fig. 7.

The related structure of $(MePh_3P^+)_2I_8^{2-}$

The crystal structure of $(MePh_3P^+)_2I_8^{2-}$ (CSD refcode ZEZDIR)[14] contains an I_8^{2-} ion with a zigzag chain of 8 iodine atoms, which is effectively two I_3^- connected by I_2. Then, the crystal structure of $(MePh_3P^+)_2I_8^{2-}$ is in effect $2 \times MePh_3P^+I_3^- + I_2$, and as such is related to the structures described in this paper. The similarity is illustrated by Fig. 10, to be compared with Fig. 1: the principal difference is that the I_2 sections of the anion provide bonded links along the *Y* crystal packing direction. Our speculative suggestion of crystal growth along the *X* direction could apply here also.

Acknowledgements

This research is supported by the Australian Research Council and the University of New South Wales. PAWD, Honorary Visiting Professor at UNSW, thanks the University of Western Ontario for a sabbatical leave.

References

1 J. D. Dunitz and J. Bernstein, *Acc. Chem. Res.*, 1995, **28**, 193–200; A. Gavezzotti, *CrystEngComm*, 2002, **4**, 343–347.
2 J. Bernstein, R. J. Davey and J.-O. Henck, *Angew. Chem., Int. Ed.*, 1999, **38**, 3441–3461.
3 A. L. Bingham, D. S. Hughes, M. B. Hursthouse, R. W. Lancaster, S. Tavener and T. L. Threlfall, *Chem. Commun.*, 2001, 603–604.
4 R. J. Davey, K. Allen, N. Blagden, W. I. Cross, H. F. Lieberman, M. J. Quayle, S. Righini, L. Seton and G. J. T. Tiddy, *CrystEngComm*, 2002, **4**, 257–264.
5 C. Horn, B. F. Ali, I. G. Dance, M. L. Scudder and D. C. Craig, *CrystEngComm*, 2000, **2**, 6–15; C. Horn, M. L. Scudder and I. G. Dance, *CrystEngComm*, 2000, **2**, 53–66; C. Horn, M. L. Scudder and I. G. Dance, *CrystEngComm*, 2001, **3**, 1–8; C. Horn, L. Berben, H. Chow, M. L. Scudder and I. G. Dance, *CrystEngComm*, 2002, **4**, 7–12.

6 F. Maharaj, V. M. Russell, M. L. Scudder, D. C. Craig and I. G. Dance, *CrystEngComm*, 2002, **4**, 149–154.
7 L. Addadi and S. Weiner, *Angew. Chem., Int. Ed. Engl.*, 1992, **31**, 153–169.
8 J. J. M. Donners, R. J. M. Nolte and N. A. J. M. Sommerdijk, *J. Am. Chem. Soc.*, 2002, **124**, 9700–9701.
9 V. Paraschiv, M. Crego-Calama, T. Ishi-i, C. J. Padberg, P. Timmerman and D. N. Reinhoudt, *J. Am. Chem. Soc*, 2002, **124**, 7638–7639.
10 H. J. Berthold and R. Wartchow, *Z. Naturforsch., B: Chem. Sci.*, 1991, **46**, 703.
11 M. Scudder and I. Dance, *J. Chem. Soc., Dalton Trans.*, 1998, 3167–3176; M. Scudder and I. Dance, *J. Chem. Soc., Dalton Trans.*, 1998, 3155–3166.
12 S. Belanger and A. L. Beauchamp, *Acta Crystallogr. Sect. C*, 1993, **49**, 388.
13 K. F. Tebbe and T. Farida, *Z. Naturforsch., B: Chem. Sci.*, 1995, **50**, 1685.
14 F. N. Tebbe, M. E. Essawi and S. A. E. Khalik, *Z. Naturforsch., B: Chem. Sci.*, 1995, **50**, 1429–1439.